

Development of a Cone CVT by SDPD and Topology Optimization

Nikhil Patil, Ehsan Malekipour, Hazim El-Mounayri

Collaborative Additive Manufacturing Research Initiative at IUPUI (CAMRI)

Purdue School of Engineering and Technology, Indianapolis, IN, USA

Abstract

The automotive industries have undergone a massive change in the last few decades. Nowadays, automotive industries and OEM manufacturers implement various innovative ideas to ensure the desired comfort while minimizing the cost, weight, and manufacturing time. Transmission system plays a major role in the aforementioned items. This paper aims to develop a conical roller with belt Continuously Variable Transmission (CVT) System by employing the System Driven Product Development (SDPD) approach and topology optimization of its traditional design. Furthermore, this paper explains the design steps of the CVT and its advantages and limitations compared with the other automatic transmission systems.

Introduction

Nowadays many automobile industries, as well as customers, consider Continuously Variable Transmission (CVT) system as the primary transmission over the conventional manual gearboxes and epicyclic gear train due to its higher fuel efficiency, wider torque range, and smoother start-up and acceleration [1,2]. CVTs work on the same principle as a conventional manual transmission system works. In other words, in a conventional transmission system, different pitch-circle diameters of the input and output gears lead to different gear ratios. Whereas the infinitive number of different diameters of the input and output pulleys/cones result in continuous torque ratios in CVT. CVT has been a popular transmission system among many automobile industries such as Nissan, Audi, Chevrolet, Honda, Ford, etc. CVT with metal pushing belt and variable pulleys is the most familiar and mostly used CVT in the current automotive industry. This type of CVT transmits the torque through a number of metal blocks, which are placed on one another and pushing each other. The variable pulleys make continuous compatibility between the engine performance map of a car and the external load. This enables the car to use the optimized function of the engine. This type of CVT significantly decreases fuel consumption and improves the acceleration compared with the traditional one [3]. However, this type of CVT suffers from the complex mechanism, distortion of the pulleys, and frequent abrasion in the pulleys surfaces. The other types of CVTs are also hampered predominantly by the low efficiency, disability to transfer high torque, and significant weight. For instances, the spherical CVT is not suitable for high torque applications because of the slippage possibility and the toroidal CVT has a complex design and thus, it has a higher manufacturing cost [4]. This paper focuses on one of the other less frequent types of CVT, known as the cone CVT. A cone CVT uses two conical rollers instead of pulleys and it transmits the power through a belt/ring. Different diameters of the conical rollers result in different torque[†] ratios. This type of CVT provides infinitive torque ratios, such as the CVT with variable pulleys, which makes it superior compared with the manual and automatic epicyclic transmission systems. The possibility of elimination of hydraulic

control system, low number of parts, simple clamping (for shifting mechanisms and control unit), low tolerance requirements, and low shifting power with electromechanical actuation are some of the advantages of the cone CVT over the one with variable pulleys. Furthermore, less manufacturing cost, easier to maintain, and a less possibility to distort due to the transmission of high torque are the other advantages [5, 6].

Börner in 2009 [5] developed the cone-ring CVT, called KRG (Fig. 1), for a wide performance spectrum. His work shows that a cone CVT can design and work in a purely mechanical approach, which makes the control system and mechanism simple and more robust, decrease the number of components, and eliminate the need to the hydraulic system. The aforementioned items significantly reduce manufacturing, maintenance, and repair costs and improve efficiency. Elimination of hydraulic pump to control the components movement shortens the unwanted delay in the shifting process of the involved dynamic systems.



Figure 1: The open KRG cone-ring CVT

The shifting mechanism in the cone CVT is much simpler than the one with variable pulleys. Fig. 2 shows one of the employed shifting mechanism for a cone CVT [5]. In this mechanism, an input cone (1), an output cone (2) are connected to each other through a transfer ring (3), which can be placed around the input or output cone. Changing the diameter and angle of the cones adopt the start-up and overdrive ratio, as well as the ratio, spread according to the vehicle requirements and installation space. The required clamping force is obtained through the axial displacement of the output cone. A mechanical torque sensor (4) transforms the output torque into an axial pressure force with very high efficiency [5]. Any cone CVT may utilize this mechanism for changing the torque ratio. However, this

[†] Corresponding author: Ehsan Malekipour (emalekip@purdue.edu)

type of CVT has not been taken into consideration for a while by scholars because of some disadvantages/drawbacks including a considerable weight and large volume of the conical roller compared with the CVT with variable pulleys or an automatic transmission system. This type of CVT also suffers from low efficiency because of the slipping issue and the limitation to transfer high torque [6]. However, its excellent benefits such as simple mechanism, less production cost, the non-hydraulic control system, etc. attract scholars and car manufacturers again nowadays. The purpose of this paper is to eliminate these limitations by introducing a new topology optimized design for the CVT and using System Driven Product Development (SDPD) (Fig. 3) methodology. Furthermore, this paper illustrates an example of product development using the SDPD approach.

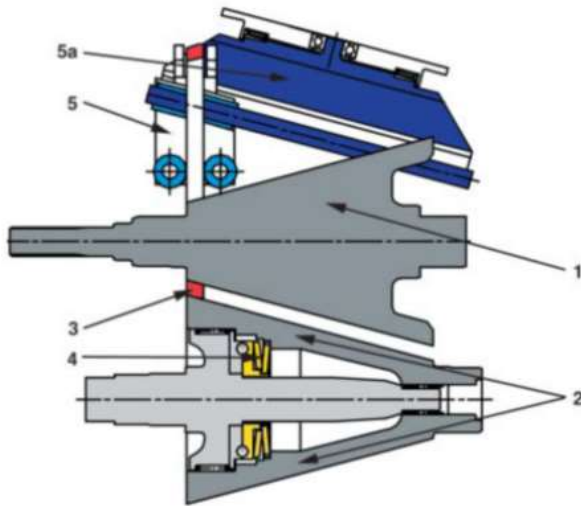


Figure 2: A designed cone-ring CVT with the shifting mechanism

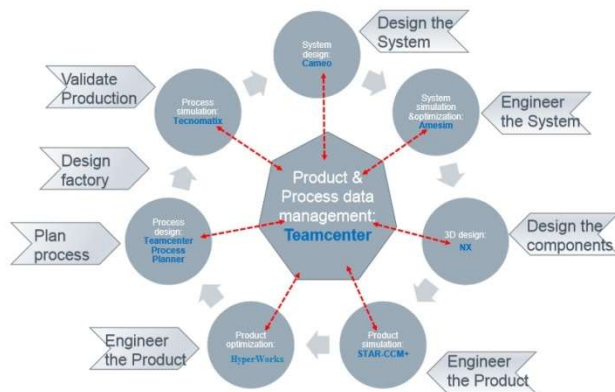


Figure 3: Different phases of the SDPD methodology

SDPD approach focuses on scaling the product development processes by eliminating the conventional document of driven product development and evolving the model-based product development [7, 8]. SDPD approach firstly uses SysML tools for developing the system, which would demonstrate the requirements of the system as well as its external and internal structure. Secondly, it uses a 1D model to simulate the behavior of a system, where you can use to validate the structure of the system. Thirdly, it uses product designing, analysis, and optimization. This phase uses CAD modeling and analysis tools. Lastly, the manufacturing process planner, plant simulation, and

manufacturing phases are included. This case study focuses on the first three phases [7].

In this study, one of the requirements of the system is the fuel economy. Our requirement is to get a better fuel economy than the existent epicyclic gear train for the cone CVT. A number of studies investigated the fuel efficiency of different types of CVT. These studies show that one of the major influencing factors for selecting a CVT system over other transmission systems is its better fuel economy because a CVT system is able to perform in the most efficient zone of Brake-specific fuel consumption (BSFC) diagram compared with transmission using fixed gear ratio [1, 9, 10].

Singh, T. and Nair, S.'s review paper corroborates the advantages of CVT over the other transmission systems. Moreover, they normalized the mathematical model of different types of CVTs and compared their efficiency with each other [11].

Previous literature shows cone CVTs have a great fuel efficiency compared with manual and automatic transmission systems as well as other CVTs systems. Srinath N. compared the efficiency and fuel consumption of the cone CVTs with the manual and automatic transmission system in his work. He showed that this type of CVT reduces the fuel consumption more than 17% compared with the manual and automatic transmission systems and the manufacturing cost will be less. However, this work used the traditional design of the cone CVT, which is suitable for a low load application. Moreover, they designed a manual mechanism with a limited range of gear ratios [12]. Recent developments in materials as well as in the optimization methodologies make possible to optimize the CVT for heavy-duty applications such as automobile industry with a functional weight and volume. In a recent project, European commission in 2017 funded a project called KRG-250 to develop a fuel efficient, cost effective cone-ring CVT for European passenger vehicles [13]. The summary of their objectives offers 30% production cost saving, 25% improved efficiency, and up to 30% reduced fuel consumption.

In this work, we try to leverage the power of SDPD methodology by the employment of some intuitive user interfaces in the field of system engineering to develop and optimize a cone CVT and overcome some of the aforementioned drawbacks/gaps in CVT transmission systems. This work exemplifies the optimization procedure by utilization of some common SE software. This procedure may follow to develop any other product and by using any other software with similar functionalities.

Problem statement

The automaker's production rate and the people's interest in various types of power transmission systems vary in different parts of the world. Many countries including India and European countries prefer a manual transmission system over an automatic one [1, 14]. An automatic transmission system has not been popular in BRIC countries (Brazil, Russia, India, and China) due to various reasons. First, because of the high cost of automatic transmission systems and their low fuel efficiency. Fuel economy has been always a significant factor for customers especially in developing countries while purchasing a car. This is the reason why only a few international automobile manufacturers offer automatic transmission systems, including CVT in these countries. Furthermore, the roads with a good condition and well-organized traffic, which allows a uniform movement with less break. Thus, the gearbox can run at a lower gear ratio for a longer period, without a need to change the gear regularly. These factors decrease the influence of using automatic transmission systems, whose fuel efficiency is less than the manual ones. However, in developing countries such as India, where the roads are not in such good condition, traffic moves at a very slow pace, and frequent downshifts are required, most domestic automakers and costumers prefer a highly economic transmission system. Even though CVT can adjust the gear ratio

input parameters and make sure that the system is able to give us the desired outputs/functions. Fig. 7 shows the simulated powertrain system in Amesim including the engine specifications, vehicle weight, generic CVT dimensions, a clutch, and some sensors as the inputs. The purpose of Amesim simulation here is to make sure that the CVT system in the designed powertrain system is going to satisfy our requirement of getting different desired torque ratios as well as provides us with a full analysis of the generated/required torque values and vehicle speeds at different CVT ratio. This can validate whether or not the CVT can provide the desired functions.

This is one major advantage of the SDPD approach; you can validate the behavior of a system even before designing the component. So, you will know whether it is worth moving forward with the idea or not. For instance, in this case study, we model the CVT structure in Cameo by virtually assembling of the system components. This assists to validate virtually if the designed system is functional and fulfills the requirements, or any additional component or modifications are required to complete the system. Amesim directs us in identifying those issues. Once, we identified all the required components by Cameo then Amesim investigates the system behavior. Amesim requires inputs just as a real car would require an input from the Engine. Engine specifications used for this example are generic. This is just to see the behavior of a system prior to designing the system. After completing the simulation, the required output parameters are derived to evaluate the system.

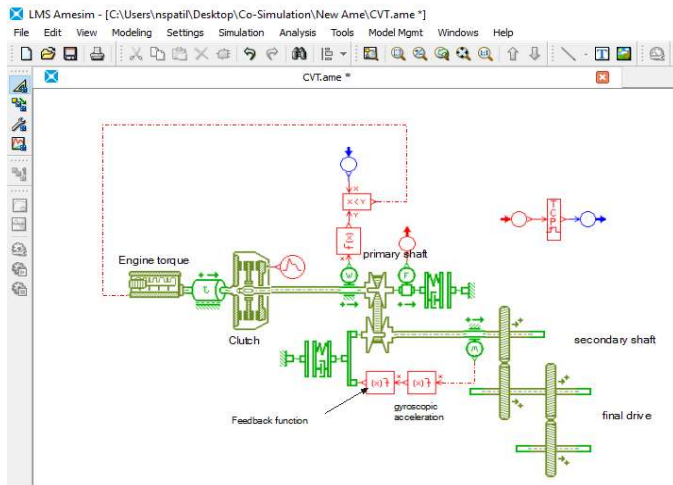


Figure 7: The powertrain system designed in LMS Amesim and the TCP elements for transferring data to the other Siemens PLM tools

Fig. 8 shows the Amesim results including the range of torque ratio that the CVT is going to generate, the forces induced on the CVT, and any other desired output associated with the designed system. These results show that the CVT fulfills the requirement.

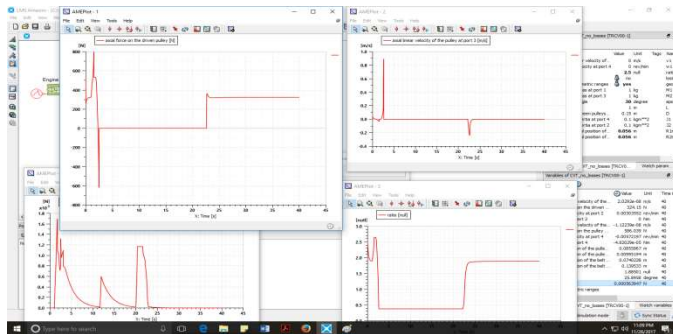


Figure 8: The Amesim results

Furthermore, employment of system engineering helps design engineers to gain the benefits from communication between such software to evaluate different aspects of the designed system. For instance, in this case study, using Amesim makes possible to transfer data to the other Siemens PLM tools such as Star CCM+. This tool enables users to perform 1D or 3D co-simulation to perform CFD or stress analysis on the corresponding component. In many cases, this stage can be repeated in a loop after designing the system to modify the design with the actual values. TCP element, shown in Fig. 7, is a crucial element for transferring the data back and forth.

Design of components: conical rollers design

The heart of the CVT system is its conical rollers. This type of transmission system uses two conical rollers, which place in front of each other with the opposite direction (Fig. 9). Fig. 10 shows the primary shape of the rollers. We optimize this part of the CVT in the following sections in order to decrease the weight of the transmission system as one of the other requirements mentioned in Cameo model. This section obtains the primary dimensions of the rollers, according to the exerted forces and other design conditions.

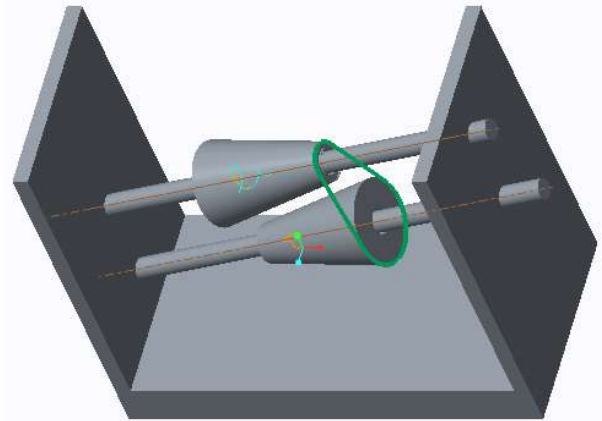


Figure 9: A CVT with a belt and conical roller modeled by Creo

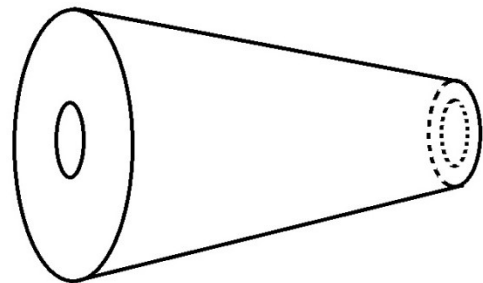


Figure 10: The primary shape of the rollers

We used the specifications of the 2013 Nissan Altima as well as the CVT characteristics achieved in the previous section, to calculate the forces and design the rollers. The vehicle specifications include the power produced by the engine, which is 82 KW and the engine RPM, which is 6000 [17]. Furthermore, the main roller dimensions by considering the optimized torque range are as follows:

- The smaller diameter of the rollers: $d = 50 \text{ mm}$
- The bigger diameter of the rollers: $D = 200 \text{ mm}$

- The length of the rollers: $L = 200$ mm

The belt exerts different force values at a different diameter of the input roller. For instance, by taking the average diameter of the roller, the velocity of the belt is:

$$v = \frac{\pi DN}{60000} \Rightarrow v = \frac{\pi \times 125 \times 6000}{60000}$$

$$\Rightarrow v = 39.26 \frac{m}{s} \quad (1)$$

In this velocity, the difference of the tight side tension of the belt (P_1) and the slack side tension (P_2) is given as:

$$P_1 - P_2 = \frac{1000(P)}{v} = \frac{1000(82)}{39.26} = 2088.11 \text{ N} \quad (2)$$

Center distance between the input shaft and output shaft (C) is equal to 150 mm. Thus, we can obtain the length of the belt:

$$L = 2C + \frac{\pi(D + d)}{2} + \frac{(D - d)^2}{4C}$$

$$L = 730.19 \text{ mm} \cong 731 \text{ mm} \quad (3)$$

We can also obtain the wrap angle for the smaller pulley by Eq. 4

$$\alpha_s = 180 - 2 \sin^{-1} \left[\frac{D-d}{2C} \right] \quad (4)$$

And the wrap angle for the bigger sized pulley by Eq. 5

$$\alpha_s = 180 + 2 \sin^{-1} \left[\frac{D-d}{2C} \right] \quad (5)$$

As it already mentioned, both rollers are identical, which places in front of each other with opposite direction. At the initial stage, the belt is in contact with the smaller end of the driving roller and the larger end of the driven roller. As the operation starts, the belt will slide along both rollers. In the case of driving roller, the belt would be sliding from the smaller end diameter to the bigger end diameter of the roller. Since the driving roller starts with the end with a smaller diameter, we would have to use the smaller roller wrap angle until it reaches the midpoint of the roller. Length of the roller is 200 mm; hence, 100 mm is its midpoint. At 100 mm length from either side, the wrap angle is 180° for both rollers. From the midpoint to the other end of the driving roller, it will have a greater diameter compared with the driven roller. In that case, the larger wrap angle is required for the driving roller. The wrap angle at the initial stage, when the belt locates at the smaller diameter of the driving roller ($d = 30$ mm) and the larger diameter of the driven roller ($D = 120$ mm), is equal to

$$\alpha_s = 180 - 2 \sin^{-1} \left[\frac{D-d}{2C} \right]$$

$$\alpha_s = 180 - 2 \sin^{-1} \left[\frac{200 - 50}{2 \times 150} \right]$$

$$\alpha_s = 120^\circ = 2.09439^c$$

We can obtain the tension on the tight side of the belt and tension on the slack side of the belt by Eq. 6:

$$\frac{F_1}{F_2} = e^{\mu \alpha_s} \quad (6)$$

Where μ is the coefficient of friction and it is considered as 0.35 [18]. Considering Eq.2, the forces can be calculated as:

$$\frac{F_1}{F_2} = 2.09439, (F_1 - F_2) = 2088.11 \text{ N}$$

$$\Rightarrow F_1 = 3996.113 \text{ N}, F_2 = 1908.003 \text{ N}$$

In order to calculate the belt tensions at different belt positions, the length of the conical roller is divided into 100 nodes with a distance of 2 mm between every two consecutive nodes. The following MATLAB code calculates the belt tensions at each corresponding node. In this code, the symbol i shows the position of the belt on the roller (from the smaller end of the conical roller), F_1 shows the belt force on the tight side, and F_2 shows the belt force on the slack side. Moreover, Alpha shows the wrap angle at the corresponding belt position, D shows the diameter of the driven conical roller wrapped by the belt, and d shows the diameter of the driving conical roller wrapped by the belt.

```
P = 82;
Do = 200;
n = 6000;
do = 50;
L = 200;
theta = atan((Do - do)/(2*L));
i = 2;
C = 150;
v = (pi * ((do+Do)/2) * n)/60000;
Force_Difference = (P * 10^3 / v);

alpha = pi - (2 * asin((Do - do)/(2 * C)));
%alpha = (alpha_degree) * pi/180;h
F2 = Force_Difference/(alpha - 1);
F1 = Force_Difference + F2;
fprintf('Initial_F1 = %d, Initial_F2 = %d', F1, F2);
while (i < 201)
    d = do + 2*(tan(theta) * i);
    D = Do - 2*(tan(theta) * i);
    v = (pi * ((d+D)/2) * n)/60000;
    Force_Difference = (P * 10^3 / v);
    if(D > d)
        alpha = pi - (2 * asin((D - d)/(2 * C)));
    else
        alpha = pi + (2 * asin((d - D)/(2 * C)));
    end
    a = alpha * (180/pi);
    F2 = Force_Difference/(alpha - 1);
    F1 = Force_Difference + F2;
    %Fx = F * cos(alpha/2);
    %Fy = F * sin(alpha/2);
    %fprintf('\n \t i = %d, \t Fx = %d, \t Fy = %d', i, Fx, Fy);
    fprintf(' \n \t i = %d, \t F1 = %d, \t F2 = %d, \t Alpha = %d, \t d = %d, \t D = %d', i, F1, F2, a, d, D);
    i = i + 5;
end
```

The results provide forces on the conical roller at different diameters. Table 1 shows some of these forces.

Table 1: Some forces of the roller obtained by the MATLAB code

i (mm)	F1 (N)	F2 (N)	Alpha °	d (mm)	D (mm)
0	3996.11	1908.11	120	50	200
5	3901.23	1813.12	123.28	53.75	196.25
10	3816.59	1728.48	126.51	57.50	192.50
15	3740.53	1652.42	129.69	61.25	188.75
20	3671.74	1583.63	132.84	65	185
100	3063.14	975.02	180	125	125
200	2742.9	654.8	240	200	50

We can obtain the final dimensions of the conical roller shown in Fig. 11 by considering the results from previous sections including the optimized torque ratio, the exerted forces, displacement limitations, and the length of the conical roller. We can find the final diameter of the shaft by substituting the torsion moment (Eq. 7) and the bending moment (Eq. 8) in Eq. 9. We selected plain Carbon Steel 40C8 with a tensile strength of 580 MPa and yield strength of 380 MPa as the material for the design of the shaft. Fig. 12 shows the final dimensions, which are 35 mm for the diameter of the shaft, 50 mm for the end of the conical roller with a small diameter, and 200 mm for the end of the conical roller with the bigger diameter.

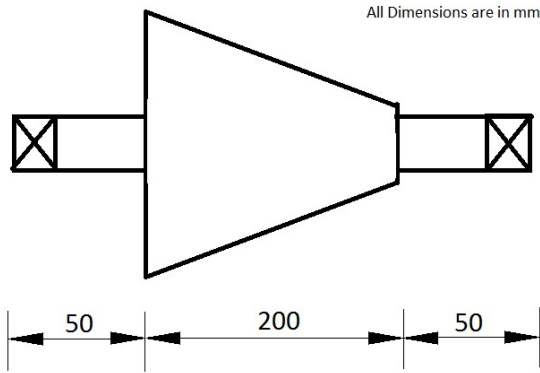


Figure 11: The layout of the input shaft

The Torsion moment is:

$$M_t = \frac{P \times 60 \times 10^6}{2\pi N} \quad (7)$$

$$\Rightarrow M_t = \frac{82 \times 60 \times 10^6}{2\pi \times 6000} \Rightarrow M_t = 130507.05 \text{ N} - \text{mm}$$

Moreover, the bending moment is:

$$M_b = (3996.11 + 1908.11) \times 100 \quad (8)$$

$$\Rightarrow M_b = 590422 \text{ N} - \text{mm}$$

Thus, the diameter of the shaft can be obtained by:

$$d_s^3 = \frac{16}{\pi \tau_{max}} \sqrt{(1.1M_t)^2 + (1.1M_b)^2} \quad (9)$$

$$\Rightarrow d_s = 31.93 \approx 32$$

By taking the standard dimension the diameter is

$$d_s = 35 \text{ mm}$$

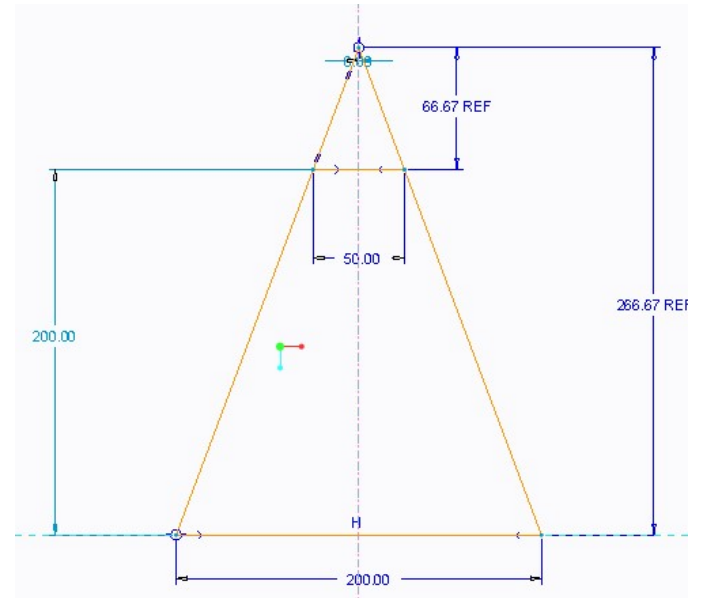


Figure 12: Dimensions of the designed conical roller

The volume of a conical roller is,

$$V = \frac{1}{3} \pi (R^2 H - r^2 h) \quad (10)$$

Where, H is the height of a cone with the base radius of 100 mm, h is the height of a cone with a base radius of 25 mm, R is the radius of the larger end of the roller, and r is the radius of the small end of the roller. Thus, the volume is obtained as,

$$V = 2618020 \text{ mm}^3 = 0.002618020 \text{ m}^3$$

By considering the density of steel equals to 7850 Kg/m³ the weight of the conical roller will be:

$$W = \rho V \quad (11)$$

$$\Rightarrow W = 20.55 \text{ Kg}$$

Table 2 compares the weight of the newly designed CVT with the previously designed CVT [12]. This weight still can be significantly improved by the employment of optimization methods. We fulfilled this objective in the next section.

Table 2: Comparison of the weight of the newly designed CVT with the traditional design

SR. No.	Volume (m ³)	Density (Kg/m ³)	Mass (Kg)
1	16 x 10 ⁻³	7850	126
2	2.6 x 10 ⁻³	7850	20.55

Design optimization

In this step, we are going to optimize the shape of the conical roller in order to reduce the weight while keeping its functionality for transferring the torque using HyperWorks-OptiStruct. We have calculated 200 forces by MATLAB exerted on 100 points at a distance of 2 mm from each other. Thus, we selected the mesh with the size of 2 mm. As Fig. 13 shows, we used tetrahedral meshes for analysis of the model. As Fig. 14 shows to the sake of a safe design, we first analyzed a roller while concentrated loads were inserted instead of the distributed load of the belt on the roller. In this case, we will have a

contact line between the roller and the belt/ring when the belt moves along the roller. Fig. 15 shows the von Mises stress analysis and Fig. 16 shows the deformation/displacement through the model. This assumption will also help in the optimization phase of the model. Our calculation shows that to transfer the torque, we need to consider at least eight contact lines throughout the roller's surface to have enough contact points between the belt/ring and the conical roller during rotation. We employed OptiStruct-HyperWorks for all the stress analysis and optimization design in this work.

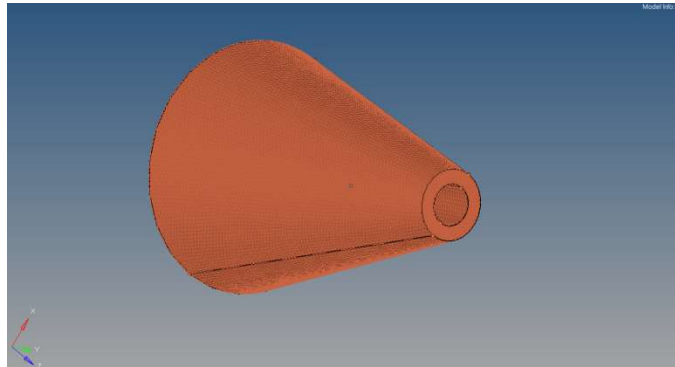


Figure 13: The meshed conical roller

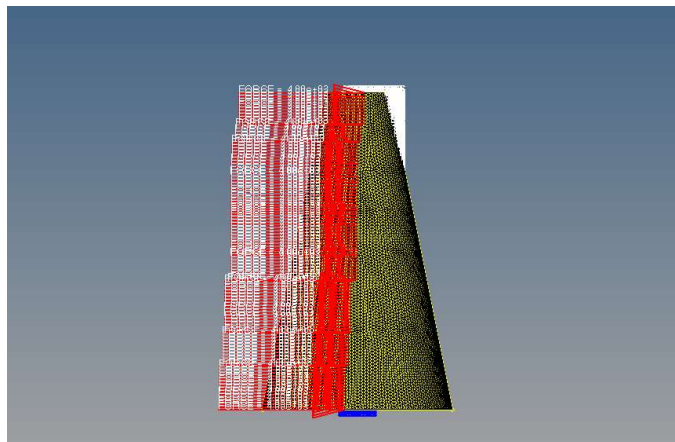


Figure 14: The applied forces on the nodes of the driving conical roller

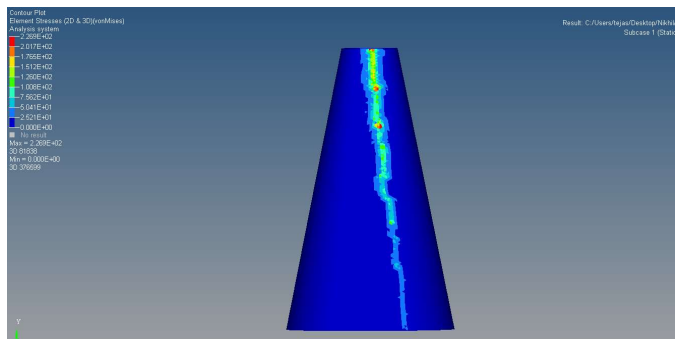


Figure 15: Von Mises stress analysis

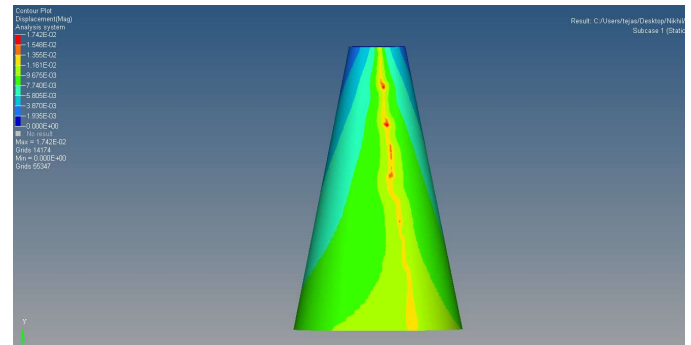


Figure 16: Deformation/displacement through the driving conical roller

Fig. 17 shows the von Mises stress analysis for the applied forces on the eight different contact lines on the driving conical roller. We assumed all the eight contact lines for analysis of the roller because the roller rotates with a very high rpm and the mechanism for moving the belt may need to change its position very quickly to change the torque ratio. Furthermore, we need all the contact points of the belts with the roller to be able to optimize the shape, the design will be safer, and the structure will be symmetric and stronger.

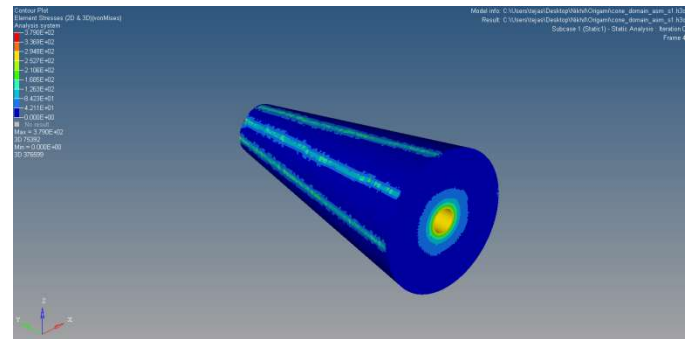


Figure 17: Von Mises stress analysis for eight contact lines

We obtained the optimized conical rollers (Fig. 18 and Fig. 19) by keeping the outer body as a non-design domain and the inner part as the design domain (Fig. 20). We employed the SIMP optimization methodology, which removed 70% of the total material of a conical roller. Thus, the ultimately generated volume became 30% of the original Volume. This new design also let to eliminate the slipping issue by designing and employing a customized belt to grab the solid outer lines (see Fig. 18). This can significantly improve the efficiency of this type of CVT and enhance the level of the torque transferred by the transmission system.

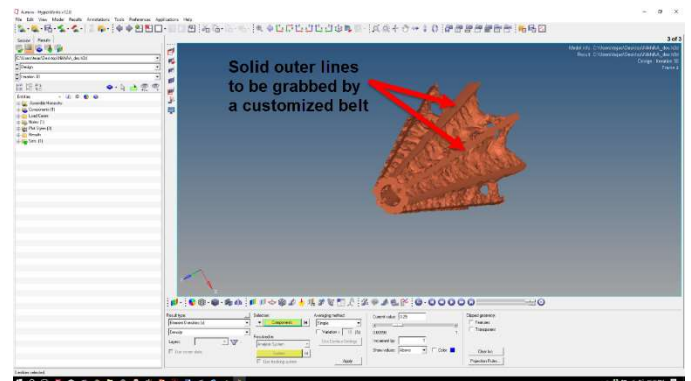


Figure 18: The optimized driving conical roller

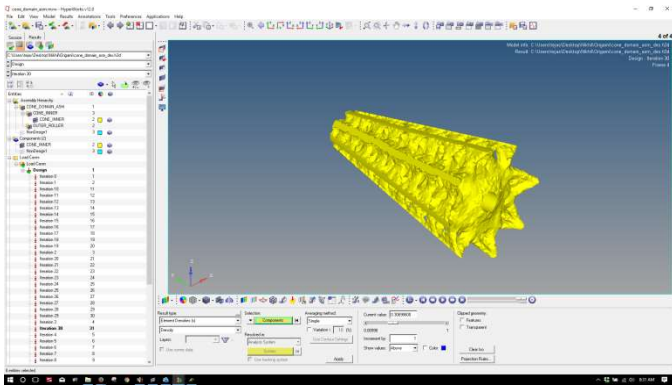


Figure 19: The optimized driven conical roller

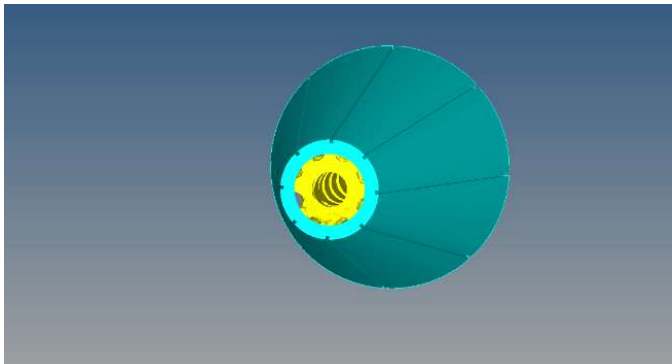


Figure 20: The non-design and design domain

We employed the high strength steel alloy, recognized as ASTM A514. Table 3 shows its specifications.

Table 3: The specifications Comparison between the conical roller before and after topology optimization

SR. No.	Volume (m ³)	V-M Stress (MPa)	Density (Kg/m ³)	S _{yt}	Mass (Kg)
1	2.6 x 10 ⁻³	231	7850	690	20.55
2	1.17 x 10 ⁻³	268	7850	690	9.185

The optimized design reduced the weight of one conical roller to 10 Kg. Thus, the total weight of the CVT system including two rollers, shafts, keys, stoppers, the mechanism for moving the belt, etc. is less than 50 kg, which satisfies the weight requirements mentioned in Cameo software.

Manufacturing feasibility

The topology-optimized conical roller possesses a freeform geometry with a complex porous structure. Traditional manufacturing processes are unable to fabricate these types of structures. Alternatively, additive manufacturing (AM) processes are capable of fabrication of complex structures with elaborate features. The automotive industry has been employed the metal AM processes such as the Direct Metal Laser Sintering (DMLS) or Selective Laser Melting (SLM) process widely. However, the defects and abnormalities generated during the fabrication process may affect the quality of the fabricated parts [19]. Thermal abnormalities such as distortion are among the most frequent defects in metal AM [20], which is crucial to avoid in the part with a high rotation speed such as the conical roller. Design of suitable temporary/permanent support structures between the fabricated layers can facilitate the conduction during the fabrication process as well as

strengthening the structure and thus, reduce the distortion. The fabricated support structures can also be optimized topologically to not affect the weight of the system significantly [21]. The other way to increase the precision and repeatability of the fabricated conical rollers is to employ online monitoring and control of the process. Several systems have been developing to monitor and/or remove the microstructural and macro-structural defects of the fabricated parts [22-26]. Specifically, the porous structures are at risk of damages more than simple solid structures [27, 28].

Scholars have tried to avoid/diminish these defects by controlling the controllable process parameters such as laser specifications or control the fabrication signatures such as melting pool specifications during the fabrication process [20, 29]. A number of scholars also attempted to derive the optimized process parameters even before printing a part by studying the effects of different parameters on the fabrication process through multi-physics simulation of the printing process [30, 31]. This paper studied the theoretical aspects and the design possibilities of the new cone CVT. The manufacturing repeatability and precision is still under question but the only way passes through AM technology. This manufacturing technology makes possible to fabricate the new design, which increases the overall efficiency of the transmission system. First, the new topology optimized design will decrease the rotational inertia of the rotating parts. Second, it will decrease the production cost and time, from the design phase to manufacturing, because of consuming less material for fabrication of the components and decreasing the total number of parts that need to be assembled.

Moreover, there is no investment in designing and fabricating the necessary tooling and fixtures. As regards to time, we can avoid the delays due to tooling that normally take several weeks of work. Delays are costly and thus, removing those leads to a significant financial benefit. The new design and the fabrication capabilities by AM also help to integrate the rotating input/output shaft with the cones/shifting mechanisms or at least reduce the number of parts by replacement of the ones which made of the same material by one integrated assembly. This will reduce or eliminate cost, time, and quality problems resulting from assembling operations [32].

Conclusion and future works

This paper demonstrates the ability of System Driven Product Development approach to developing an optimized cone CVT system. The existing CVT designs suffer from a number of disadvantages including the considerable weight of the conical rollers and a limited range of the torque in the cone CVT system, and complex mechanism and high production cost in other CVT types. This work employed an innovative system development approach, SDPD, to develop the cone CVT by defining desired system requirements and evaluating these requirements through predicting system behavior and designing the multi-domain system, before designing the components. The newly designed conical roller, as a major component of the CVT, was optimized using OptiStruct-HyperWorks® software. The optimized rollers result in a significant reduction in weight. Our new design could decrease the weight of the traditional cone CVT by 44.69%. This is while the literature demonstrates a non-topology optimized cone CVT can improve the efficiency by 25%, fuel efficiency by 30% and the production cost by 30%. The new design can surpass the weight efficiency of the current transmission systems in the event that other parts of the CVT system are optimized. Furthermore, it increases the efficiency of the transmission system even more by introducing a new design for the elimination of the slipping issue, reducing the rotational inertia of the rotating components, decreasing the production cost, and decreasing the assembling time. The new design results in an optimum strength-to-weight ratio able to meet functional requirements while minimizing material volume. As the future step, we can optimize the

performance of the CVT system by extending the range of the torque ratio while imposing a weight constraint on the design. The manufacturing feasibility with a high precision machining is questionable but metal AM (Additive Manufacturing) provides a unique way of fabricating the complex structures of the proposed design.

References

1. Pour, E.M. and Golabi, S.I., 2014. Examining the Effects of Continuously Variable Transmission (CVT) and a new mechanism of planetary gearbox of CVT on Car Acceleration and Fuel Consumption. *International Journal of Application or Innovation in Engineering & Management (IJAIEEM)*.
2. Giacomo Mantriota, 'Fuel consumption of a vehicle with power split CVT system', Int. J. Vehicle Design, Vol. 37, No. 4, pp.327-342.
3. Maleki Pour, E., and Golabi, S., 2014. Design of continuously variable transmission (CVT) with metal pushing belt and variable pulleys. *International Journal of Automotive Engineering*, 4(2), pp.699-717.
4. Ashish Singla, Baltej Singh Rupala, Gurvinder Singh Virk, "Optimization of stepped-cone CVT for lower-limb exoskeletons", ScienceDirect Volume 8, September 2016, Pages 592-595
5. Börner, M., 2004. The Cone Ring CVT. *AutoTechnology*, 4(2), pp.66-69
6. Seidl, M., 2011. Bachelor Thesis Continuously Variable Transmission. Bachelor of Engineering (Mechatronics), Applied Mechanics Department, Cranfield University
7. "Siemens PLM - System Driven Product Development (SDPD) Overview & Update", Mark Sampson; Pascal Vera; Business Process Connection: System Driven Product Development
8. Won Hyun Oh, Jung Hee Lee, Hyoung Geun Kwon, and Hyoung Jin Yoon, 'Model-Based Development of Automotive Embedded Systems: A Case of Continuously Variable Transmission (CVT)', Automotive Electronics R&D Center, Hyundai Motor Company & Kia Motors Corporation, IEEE
9. G. Carbone and L. Mangialardi, (2002) 'Fuel consumption of a mid class Vehicle with Infinitely Variable Transmission', SAE Transaction, Journal of Engines, Vol. 110, No. 3, pp.2474-2483.
10. L. Mangialardi and G. Mantriota, 'Power flows and efficiency in infinitely variable transmission', Mechanism and Machine Theory 34 (1999) 973-994
11. Singh, T. and Nair, S., "A Mathematical Review and Comparison of Continuously Variable Transmissions," SAE Technical Paper 922107, 1992, <https://doi.org/10.4271/922107>
12. Srinath N., 'Cone Type CVT with High Speed Variations', International Journal of Scientific & Engineering Research, Volume 6, Issue 7, July-2015
13. GIF ENTWICKLUNGSGESELLSCHAFT MBH, 2017. A fuel saving, emission reducing and cost effective Continuously Variable Transmission for European passenger vehicles. European Commission, Horizon 2020, Germany.
14. <https://www.quora.com/Why-hasnt-automatic-transmission-in-cars-become-popular-in-India>
15. M. Boos and H. Mozer, "ECOTRONIC – The Continuously Variable ZF Transmission (CVT)," *Automotive and Transport Technology Congress*, 1997.
16. Arjen Brandsma, Jan van Lith, Emery Hendriks Van Doorne's Transmissie b.v., 'Push belt CVT developments for high power applications', International Congress 99 on Continuously Variable Power Transmission CVT'.
17. <http://www.autoguide.com/manufacture/nissan/2013-nissan-ultima-review-2022.html>
18. V. B. Bhandari, 2010, Design of Machine Elements Third Edition, Tata McGraw Hill Education Pvt Ltd.
19. Malekipour, E. and El-Mounayri, H., 2018. Defects, Process Parameters and Signatures for Online Monitoring and Control in Powder-Based Additive Manufacturing. In *Mechanics of Additive and Advanced Manufacturing, Volume 9* (pp. 83-90). Springer, Cham.
20. Malekipour, E. and El-Mounayri, H., 2018. Common defects and contributing parameters in powder bed fusion AM process and their classification for online monitoring and control: a review. *The International Journal of Advanced Manufacturing Technology*, 95(1-4), pp.527-550.
21. Malekipour, E., Tovar, A. and El-Mounayri, H., 2018. Heat Conduction and Geometry Topology Optimization of Support Structure in Laser-Based Additive Manufacturing. In *Mechanics of Additive and Advanced Manufacturing, Volume 9* (pp. 17-27). Springer, Cham.
22. Barker, K., Berry, D., and Rainwater, C., A review of machine learning approaches for high dimensional process monitoring.
23. Amini, M. and Chang, S., 2018, June. Process Monitoring of 3D Metal Printing in Industrial Scale. In *ASME 2018 13th International Manufacturing Science and Engineering Conference* (pp. V001T01A035-V001T01A035). American Society of Mechanical Engineers.
24. Amini, M. and Chang, S.I., 2018. MLCPM: A process monitoring framework for 3D metal printing in industrial scale. *Computers & Industrial Engineering*, 124, pp.322-330.
25. Imani, F., Gaikwad, A., Montazeri, M., Rao, P., Yang, H. and Reutzel, E., 2018, June. Layerwise in-process quality monitoring in laser powder bed fusion. In *ASME 2018 13th International Manufacturing Science and Engineering Conference* (pp. V001T01A038-V001T01A038). American Society of Mechanical Engineers.
26. Montazeri, M., Yavari, R., Rao, P., and Boulware, P., 2018. In-process Monitoring of Material Cross-Contamination Defects in Laser Powder Bed Fusion. *Journal of Manufacturing Science and Engineering*.
27. Imani, F., Gaikwad, A., Montazeri, M., Rao, P., Yang, H. and Reutzel, E., 2018. Process Mapping and In-Process Monitoring of Porosity in Laser Powder Bed Fusion Using Layerwise Optical Imaging. *Journal of Manufacturing Science and Engineering*, 140(10), p.101009.
28. Chen, Z., Niazi, S., Zhang, G. and Bobaru, F., 2017. Peridynamic Functionally Graded and Porous Materials: Modeling Fracture and Damage. *Handbook of Nonlocal*

Continuum Mechanics for Materials and Structures, pp.1-35.

29. Montazeri, M. and Rao, P., 2018. Sensor-Based Build Condition Monitoring in Laser Powder Bed Fusion Additive Manufacturing Process Using a Spectral Graph Theoretic Approach. *Journal of Manufacturing Science and Engineering*, 140(9), p.091002.
30. Morsali, S., Daryadel, S., Zhou, Z., Behroozfar, A., Baniasadi, M., Moreno, S., Qian, D. and Minary-Jolandan, M., 2017. Multi-physics simulation of metal printing at micro/nanoscale using meniscus-confined electrodeposition: Effect of nozzle speed and diameter. *Journal of Applied Physics*, 121(21), p.214305.
31. Morsali, S., Daryadel, S., Zhou, Z., Behroozfar, A., Qian, D. and Minary-Jolandan, M., 2017. Multi-physics simulation of metal printing at micro/nanoscale using meniscus-confined electrodeposition: Effect of environmental humidity. *Journal of Applied Physics*, 121(2), p.024903.
32. Atzeni, E. and Salmi, A., 2012. Economics of additive manufacturing for end-usable metal parts. *The International Journal of Advanced Manufacturing Technology*, 62(9-12), pp.1147-1155.

Contact Information

Nikhil Patil, Quality Engineer, Union City. Research fields: Systems Engineering, Quality Control, and Solid Mechanics. Email address: nspatil@iu.edu

Corresponding author: *Ehsan Malekipour*, Research Associate, CAMRI research group, Purdue School of Engineering and Technology. Research fields: additive manufacturing, online monitoring and control, topology optimization, and design of transmission systems. Email address: emalekip@purdue.edu

Hazim El-Mounayri, Associate professor, Purdue School of Engineering and Technology, Research fields: System Engineering, Advanced and Additive Manufacturing, Nanotechnology. Phone number: [\(317\) 278-3320](tel:(317)278-3320)

Definitions/Abbreviations

AM	Additive Manufacturing
BRIC	Brazil, Russia, India, and China
BSFC	Brake-Specific Fuel Consumption
CFD	Computational Fluid Dynamics
CVT	Continuously Variable Transmission
DMLS	Direct Metal Laser Sintering
MBSE	Model Based Systems Engineering
PLM	Product Lifecycle Management
SLM	Selective Laser Melting
SPDP	System Driven Product Development
TCP	Transmission Control Protocol